

Mixed convection on a vertical surface with a prescribed heat flux: the solution for small and large Prandtl numbers

J.H. MERKIN¹, I. POP² and T. MAHMOOD³

¹*Department of Applied Mathematics, University of Leeds, Leeds LS2 9JT, UK;* ²*Faculty of Mathematics, University of Cluj, R-3400 Cluj, CP 253, Romania;* ³*Department of Mathematics, Islamia University, Bahawalpur, Pakistan*

Received 27 March 1990; accepted in revised form 20 August 1990

Abstract. The mixed convection boundary-layer flow over a vertical surface with a prescribed surface heat flux is considered for both large and small values of the Prandtl number. The similarity equations are treated first. It is shown that, for large values of the Prandtl number, the solution approaches the forced convection limit with the free convection effects having only a small perturbation on this. The opposite is seen to be the case for small values of the Prandtl number, now free convection becomes the dominant heat transfer mechanism. A consequence of this is seen to be that the range of negative buoyancy parameter (opposed flow) over which a solution can exist decreases to zero as the Prandtl number is decreased.

The scalings worked out for the similarity equations are then applied to the general boundary-layer flow, with the particular example of a uniform stream over a flat plate with uniform surface heat flux being treated in detail. Again it is seen that, for large Prandtl numbers, the solution approaches the forced convection limit whereas, for small Prandtl numbers, free convection dominates the flow. The effect of this is seen, for opposed flow, to delay the onset of separation for large Prandtl numbers, and to bring the separation point closer to the leading edge as the Prandtl number is decreased. An estimate for this effect is obtained.

1. Introduction

The importance of the Prandtl number in determining the nature of the flow and heat transfer in free convection boundary layers was recognised from the outset [1, 2, 3]. Consequently there have been several studies in which this effect has been analysed in some detail. Lefevre [4] was the first to write down the leading terms of the inner and outer expansions for both small and large Prandtl numbers. At the same time a solution for large Prandtl number was obtained by Stewartson and Jones [5] for the flow on an isothermal vertical plate. They showed that in this case the boundary layer divides up into two regions; there is an inner region in which the temperature decreases from its value on the plate to that of the ambient fluid and a much thicker outer region in which the fluid is at its ambient temperature and which is driven by the flow in the inner region. This work was later extended by Kuiken [6] and Eshghy [7]. The solution in this limit when a constant heat flux boundary condition is applied has been treated by Roy [8].

At the other end of the Prandtl number range, Kuiken [9] has derived the solution for the free convection boundary on an isothermal vertical plate valid for small Prandtl numbers. Here the boundary layer again divides up into two regions, but now the inner region is, to leading order, isothermal (at the same temperature as the plate) with a thicker outer region at the outer edge of which the ambient conditions are attained. This work has been extended by Merkin [10] for the case of a prescribed surface heat flux boundary condition. Here the situation is basically the same as that seen in [9], though the scalings for the two regions are

different and the temperature of the inner region is now determined through the matching with the outer region.

The original work on mixed convection flows on vertical surfaces by Sparrow and Gregg [11], Szewczyk [12] and Merkin [13], for isothermal surfaces, and by Wilks [14, 15] for a uniform surface heat flux, established the basic flow structure by joining an essentially forced convection solution near the leading edge to an essentially free convection solution far downstream (for aiding flows) and by describing the nature of the boundary-layer separation (for opposing flows). This work concentrated on results for Prandtl numbers of order unity, with there being little previous work on describing the structure of these flows when the Prandtl number is either large or small. It is the purpose of this paper to consider this aspect in more detail. In particular we consider the mixed convection boundary-layer flow on a body with prescribed surface heat flux. We begin by discussing the similarity equations for this problem. These have been treated previously in some detail by Merkin and Mahmood [16] for Prandtl numbers of order unity. Here we examine the behaviour of their solution for both small and large Prandtl numbers. We find that in the large Prandtl number limit the flow approaches that for purely forced convection, with the effects of free convection being a small perturbation on this. For small Prandtl numbers the situation is reversed, now the leading order solution is the corresponding free convection flow with the contribution from the free stream being a perturbation on this. These ideas are then extended to general boundary-layer flows. As a particular example, we consider in detail the flow of a uniform free stream over a uniformly heated vertical plate; a problem which has been discussed for Prandtl numbers of order unity by Wilks [14, 15] and Hunt and Wilks [17]. Here we extend the results given in [14, 15] to both small and large Prandtl numbers.

2. Equations

The equations governing the steady two-dimensional mixed convection boundary-layer flow of a free stream $\bar{U}(\bar{x})$ over a vertical surface are

$$\frac{\partial \bar{u}}{\partial \bar{x}} + \frac{\partial \bar{v}}{\partial \bar{y}} = 0, \quad (1a)$$

$$\bar{u} \frac{\partial \bar{u}}{\partial \bar{x}} + \bar{v} \frac{\partial \bar{u}}{\partial \bar{y}} = g\beta(\bar{T} - T_0) + \bar{U} \frac{d\bar{U}}{d\bar{x}} + \nu \frac{\partial^2 \bar{u}}{\partial \bar{y}^2}, \quad (1b)$$

$$\bar{u} \frac{\partial \bar{T}}{\partial \bar{x}} + \bar{v} \frac{\partial \bar{T}}{\partial \bar{y}} = \nu/\sigma \frac{\partial^2 \bar{T}}{\partial \bar{y}^2}, \quad (1c)$$

where \bar{x} and \bar{y} are co-ordinates along and normal to the body surface respectively with \bar{u} and \bar{v} being the velocity components in the \bar{x} and \bar{y} directions respectively. \bar{T} is the temperature of the fluid with ambient temperature T_0 , g is the acceleration due to gravity, β is the coefficient of thermal expansion, ν is the kinematic viscosity and σ the Prandtl number. The boundary conditions to be applied are

$$\bar{u} = \bar{v} = 0, \quad k \frac{\partial \bar{T}}{\partial \bar{y}} = -\bar{q}(\bar{x}) \quad \text{on } \bar{y} = 0, \quad (2a)$$

$$\bar{u} \rightarrow U(\bar{x}), \quad \bar{T} \rightarrow T_0 \quad \text{as } \bar{y} \rightarrow \infty. \quad (2b)$$

Equations (1) and (2) can be made non-dimensional by writing

$$\begin{aligned} \bar{u} &= U_0 u, & \bar{v} &= \text{Re}^{-1/2} U_0 v, & \bar{x} &= lx, & \bar{y} &= l \text{Re}^{-1/2} y, \\ \bar{T} - T_0 &= \frac{q_0}{k} l \text{Re}^{-1/2} T, & \bar{U} &= U_0 U, & \bar{q} &= q_0 q, \end{aligned} \tag{3}$$

where U_0 and q_0 are scales for the free stream and prescribed wall heat flux respectively and l is a length scale for the body. Re is the Reynolds number, given by $\text{Re} = U_0 l / \nu$. Using (3) equations (1) become

$$\frac{\partial u}{\partial x} + \frac{\partial v}{\partial y} = 0, \tag{3a}$$

$$u \frac{\partial u}{\partial x} + v \frac{\partial u}{\partial y} = \alpha T + U \frac{dU}{dx} + \frac{\partial^2 u}{\partial y^2}, \tag{3b}$$

$$u \frac{\partial T}{\partial x} + v \frac{\partial T}{\partial y} = \frac{1}{\sigma} \frac{\partial^2 T}{\partial y^2}, \tag{3c}$$

with boundary conditions (2) becoming

$$u = v = 0, \quad \frac{\partial T}{\partial y} = -q(x) \quad \text{on } y = 0, \tag{4}$$

$$u \rightarrow U(x), \quad T \rightarrow 0 \quad \text{as } y \rightarrow \infty. \tag{5}$$

$\alpha = g\beta q_0 l^2 \text{Re}^{-1/2} / (kU_0^2)$ is the buoyancy parameter which can be written in terms of the Grashof number $\text{Gr} = g\beta q_0 l^4 / (k\nu^2)$ as $\alpha = \text{Gr} / \text{Re}^{-5/2}$.

Equations (3) admit a similarity solution if

$$U(x) = x^m, \quad q(x) = x^{(5m-3)/2} \tag{6a}$$

with then

$$\psi = x^{(m+1)/2} f(\eta), \quad T = x^{2m-1} \theta(\eta), \quad \eta = yx^{1-2m} \tag{6b}$$

where ψ is the stream function. Using (6a) and (6b), equations (4) become

$$f''' + \alpha\theta + \frac{1}{2}(m+1)ff'' + m(1-f'^2) = 0, \tag{7a}$$

$$\theta'' + \sigma \left(\frac{1}{2}(m+1)f\theta' + (1-2m)f'\theta \right) = 0, \tag{7b}$$

with boundary conditions

$$f(0) = 0, \quad f'(0) = 0, \quad \theta'(0) = -1, \quad f' \rightarrow 1, \quad \theta \rightarrow 0 \quad \text{as } \eta \rightarrow \infty, \tag{8}$$

(primes denote differentiation with respect to η) Equations (7) have been discussed previously for values of the Prandtl number of order unity by Merkin and Mahmood [16]; in

fact in [16] results were given for $\sigma = 1$. Also, it was shown in [16] that equations (7) possess a solution only if $m > \frac{1}{5}$, and we will assume throughout that this condition is satisfied.

We start by considering the behaviour of the similarity equations (7) for both small and large values of σ . This gives us an insight into how a general boundary-layer flow, as given by equations (3), will behave for small and large Prandtl numbers, which we then discuss in relation to the specific example of a uniform stream with uniform surface heat flux.

3. Similarity equations

(a) Solution for large Prandtl number

Here we expect the boundary layer to divide up into two regions, with a thin inner thermal region and an outer region at the same temperature as the ambient fluid and driven by the free stream flow. A balance of the terms in equation (7b) and boundary condition (8) then suggests that for the inner region we should put

$$f = \sigma^{-n} F, \quad \theta = \sigma^{-n} H, \quad \zeta = \sigma^n \eta, \tag{9}$$

for some constant n to be determined. Using (9), equation (7a) then reduces to $F''' = 0$ (to leading order), giving $F = \frac{1}{2} a_0 \zeta^2$, for some constant a_0 . This then gives f of $O(\sigma^{3n-1})$ and as it is readily shown that the outer region is described in the terms of original variables, we must have $n = \frac{1}{3}$. Hence the thin thermal layer has a thickness of $O(\sigma^{-1/3})$ and in it the fluid temperature is small, of $O(\sigma^{-1/3})$. These scalings for the mixed convection case (with α of $O(1)$) are different to those derived by Roy [8] for the corresponding free convection problem.

To proceed we write, in the inner layer,

$$f = \sigma^{-2/3} F, \quad \theta = \sigma^{-1/3} H, \quad \zeta = \sigma^{1/3} \eta, \tag{10}$$

with equations (7) becoming

$$F''' + \sigma^{-1/3} m + \sigma^{-2/3} \alpha H + \sigma^{-1} \left(\frac{1}{2} (m+1) F F'' - m F'^2 \right) = 0, \tag{11a}$$

$$H'' + \frac{1}{2} (m+1) F H' + (1-2m) F' H = 0, \tag{11b}$$

with boundary conditions,

$$F(0) = 0, \quad F'(0) = 0, \quad H'(0) = -1. \tag{12}$$

Primes now denote differentiation with respect to ζ and the outer boundary conditions are relaxed at this stage.

Equation (11) suggests looking for a solution by expanding,

$$F(\zeta; \sigma) = F_0(\zeta) + \sigma^{-1/3} F_1(\zeta) + \dots, \tag{13a}$$

$$H(\zeta; \sigma) = H_0(\zeta) + \sigma^{-1/3} H_1(\zeta) + \dots, \tag{13b}$$

At leading order we obtain,

$$F_0''' = 0, \tag{14a}$$

and hence,

$$F_0 = \frac{a_0}{2} \zeta^2. \tag{14b}$$

Using (14b), we obtain from equation (11b),

$$H_0'' + \frac{1}{4} (m + 1) a_0 \zeta^2 H_0' + (1 - 2m) a_0 \zeta H_0 = 0. \tag{15}$$

Equation (15) has a solution which can be expressed in terms of confluent hypergeometric functions [18] as

$$H_0 = \left(\frac{12}{a_0(m+1)} \right)^{1/3} \frac{\Gamma\left(\frac{2}{3} \left(\frac{5m-1}{m+1} \right)\right)}{3\Gamma\left(\frac{2}{3}\right)} e^{-s} U\left(\frac{2}{3} \left(\frac{5m-1}{m+1} \right); \frac{2}{3}; s\right), \tag{16}$$

where $s = \frac{1}{12} a_0 (m + 1) \zeta^3$. The arbitrary constant a_0 will be determined by the matching with the outer region. Note that (16) requires that a_0 be positive, which we will show to be the case for all $m > \frac{1}{3}$.

The solution can be extended to $O(\sigma^{-1/3})$, at which stage we obtain

$$F_1''' + m = 0, \tag{17a}$$

giving

$$F_1 = a_1 \frac{\zeta^2}{2} - m \frac{\zeta^3}{6}, \tag{17b}$$

for some further constant a_1 .

We can now turn to the outer region. Since the temperature, as given by (16), has exponential decay at the outer edge of the inner layer, (we can see that this will also be the case for the higher-order terms in expansion (13) for H), this outer region will effectively be isothermal (at the same temperature as the ambient fluid) and will have f and η left unscaled. Hence the equation governing the outer region will be equation (7a), with the term $\alpha\theta$ put to zero. The boundary conditions are that

$$f' \rightarrow 1 \quad \text{as } \eta \rightarrow \infty, \tag{18a}$$

and, from matching with the inner region, that

$$f \sim \left(\frac{a_0}{2} \eta^2 - m \frac{\eta^3}{6} + \dots \right) + \sigma^{-1/3} (a_1 \eta^2 + \dots) + \dots \tag{18b}$$

for small η . (18b) suggests looking for a solution by expanding,

$$f(\eta; \sigma) = f_0(\eta) + \sigma^{-1/3} f_1(\eta) + \dots \tag{19}$$

At leading order we obtain

$$f_0''' + \frac{1}{2} (m + 1) f_0 f_0'' + m(1 - f_0'^2) = 0 \tag{20a}$$

with

$$f_0 \sim \frac{a_0}{2} \eta^2 + \dots, \text{ for } \eta \ll 1 \text{ and } f_0' \rightarrow 1 \text{ as } \eta \rightarrow \infty. \tag{20b}$$

The problem given by (20a, b) is just the Falkner–Skan problem for the free stream $U(x) = x^m$, the solution of which, for a given value of m , determines the constant a_0 . We also note that for the values of m being considered, i.e. $m > \frac{1}{5}$, the solution of (20a, b) will have $a_0 > 0$ as required. Having obtained the leading-order solution, the higher-order terms in expansion (19) can then be computed. This need not be pursued any further here.

From (10), (14b) and (16), we then have, for $\sigma \gg 1$,

$$f''(0) = a_0 + O(\sigma^{-1/3}), \tag{21a}$$

$$\theta(0) = \sigma^{-1/3} \left(\frac{\Gamma(\frac{1}{3})}{3\Gamma(\frac{2}{3})} \frac{\Gamma(\frac{2}{3} \frac{5m-1}{m+1})}{\Gamma(\frac{11m-1}{3(m+1)})} \left(\frac{12}{a_0(m+1)} \right)^{1/3} + O(\sigma^{-1/3}) \right). \tag{21b}$$

To check the validity of this asymptotic solution, we calculated $f''(0)$ and $\theta(0)$ by numerically integrating equations (7) for increasing values of σ and compared these numerically determined values with the asymptotic forms (21). We took $m = \frac{3}{5}$ (corresponding to a uniform wall heat flux) and values of $\alpha = -0.4, 1.0$ and 5.0 . Note that for $m = \frac{3}{5}$, $a_0 = 0.97532$ and hence

$$f''(0) = 0.9753 + \dots, \quad \theta(0) = 1.5835 \sigma^{-1/3} + \dots \tag{21c}$$

Values of $f''(0)$ and $\theta(0)$ obtained by solving equations (7) numerically are shown in Figs 1 and 2 respectively (by the full lines) and from the asymptotic forms (21c) (by the broken lines). These figures show that the above asymptotic values are approached for large σ for the values of α chosen.

We note also that $f''(0)$ approaches its asymptotic value from above for the positive values of α and from below for the negative values of α . This is to be expected, as for $\alpha > 0$, free convection is aiding the boundary-layer development with a consequent increase in skin friction above the purely forced convection value (which is as shown above the large Prandtl number limit). For $\alpha < 0$ the buoyancy forces oppose the boundary-layer development and hence reduce the skin friction below the forced convection value. The opposite is the case for the wall temperature. The increased flow rate close to the wall for $\alpha > 0$ has the effect of reducing the temperature of the fluid close to the wall (for a given heat input through the wall) and hence the asymptotic value is approached from below. While, for $\alpha < 0$, the fluid velocity near the wall is reduced, giving an increase in the wall temperature and conse-

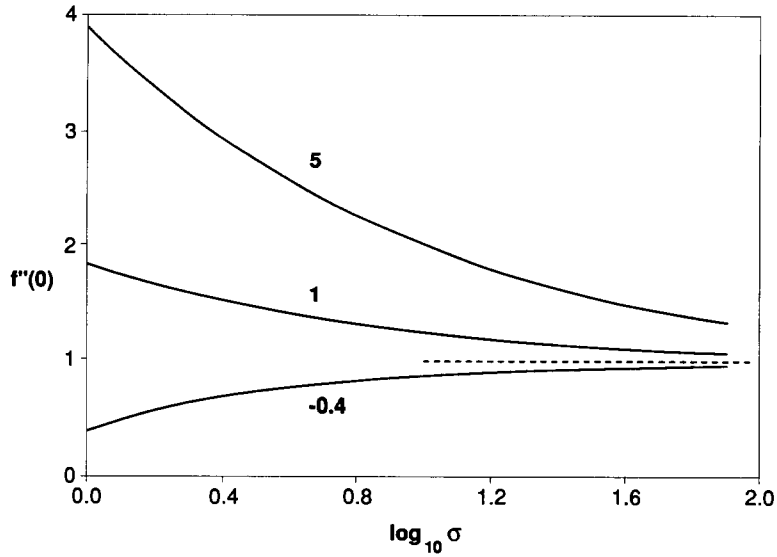


Fig. 1. A plot of $f''(0)$ obtained from the numerical solution of equations (7) for $m = 3/5$ and $\alpha = -0.4, 1.0$ and 5.0 (shown by the full lines). The asymptotic result for large σ , given by (21c), is shown by the broken line.

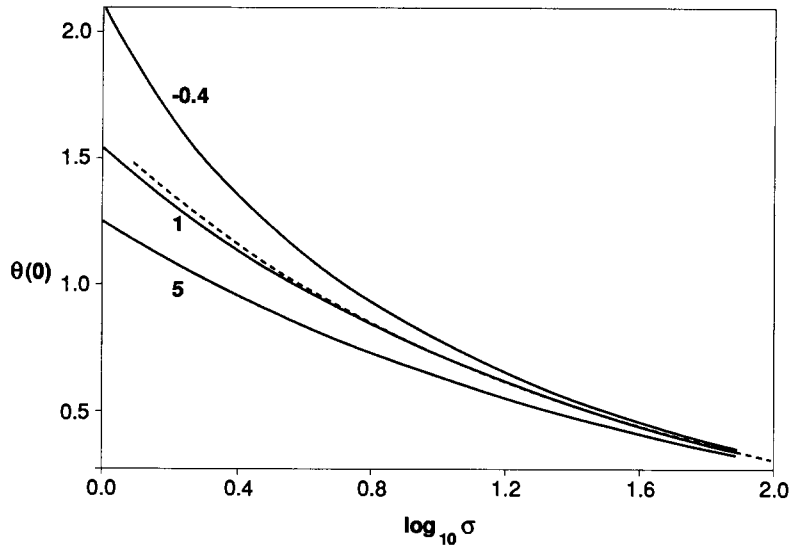


Fig. 2. A plot of $\theta(0)$ obtained from the numerical solution of equations (7) for $m = 3/5$ and $\alpha = -0.4, 1.0$ and 5.0 (shown by the full lines). The asymptotic result for large σ , given by (21c), is shown by the broken line.

quently the asymptotic (forced convection) limit is approached from above. These effects can be clearly seen also in the results presented in [16] for the case when $\sigma = 1$.

The above theory has been worked out on the assumption that α is of $O(1)$, and has to be modified when α is large. From equation (11a) we can see that the buoyancy force term will affect the leading order equation in the inner region when α is of $O(\sigma^{2/3})$. Then, putting $\alpha = \alpha_0 \sigma^{2/3}$, where α_0 is of $O(1)$, equation (11a) gives, at leading order, $F_0''' + \alpha_0 H_0 = 0$, which, together with equation (11b), has to be solved, now subject to the condition that

$F_0'' \rightarrow 0$ as $\zeta \rightarrow \infty$. This system can then be rendered independent of α_0 by the re-scaling $F_0 = \alpha_0^{1/5} \bar{F}_0$, $H_0 = \alpha_0^{-1/5} \bar{H}_0$, $\bar{\zeta} = \alpha_0^{1/5} \zeta$. The outer boundary condition has $\bar{F}_0 \sim C_0 \bar{\zeta}$ as $\bar{\zeta} \rightarrow \infty$, for some constant C_0 independent of α_0 , thus requiring an outer region in which $f = \sigma^{-1/6} f^*$, $\eta^* = \sigma^{-1/6} \eta$ and $\theta \equiv 0$. The resulting equation (when this transformation has been applied to equation (7a)), satisfying $f^* \sim C_0 \alpha_0^{2/5} \eta^*$ for $\eta^* \ll 1$, can also be rendered independent of α_0 by the scaling $f^* = \alpha_0^{1/5} \bar{f}^*$, $\bar{\eta}^* = \alpha_0^{1/5} \eta^*$. Thus the free convection limit for large σ can be obtained, wholly independent of the parameter α_0 .

Now, to obtain the free convection limit from equations (7) we apply the transformation $f = \alpha^{1/5} \bar{f}$, $\theta = \alpha^{-1/5} \bar{\theta}$, $\bar{\eta} = \alpha^{1/5} \eta$ and then let $\alpha \rightarrow \infty$ in the resulting equations. However, if we write $\alpha_0 = \alpha \sigma^{-2/3}$ in the above scalings for α and σ large problem, we obtain, using (10), an inner region in which f is of $O(\sigma^{-4/5} \alpha^{1/5})$, θ is of $O(\sigma^{-1/5} \alpha^{-1/5})$ with thickness of $O(\sigma^{-1/5} \alpha^{-1/5})$ and an outer region in which f is of $O(\sigma^{-3/10} \alpha^{1/5})$ with thickness of $O(\sigma^{3/10} \alpha^{-1/5})$. Thus, taken with the above transformation for $\alpha \gg 1$, the scalings for the free convection problem given by Roy [8] are recovered, and the limit that $\alpha \ll \sigma^{2/3}$ for the previous theory to be valid is obtained.

(b) *Solution for small Prandtl number*

The solution for the related free convection problem [10] suggests that for small Prandtl number the boundary layer will again divide up into two regions, with there being an inner isothermal region next to the wall and an outer inviscid region. To obtain the scalings for the two regions we note that, for the inner region, the viscous, buoyancy and convective terms in equation (7a) must balance, suggesting that we write

$$f = \sigma^r \phi, \quad \theta = \sigma^{4r} g, \quad \tau = \sigma^r \eta, \tag{22a}$$

where ϕ , g and τ are all of $O(1)$ in the inner layer and r has to be determined. Using (22a), equation (7b) reduces to $g'' = O(\sigma)$ and boundary condition (8) gives $g'(0) = -\sigma^{-5r}$ (primes now denote differentiation with respect to τ). Then, assuming for the moment that $r < 0$ and $-5r < 1$, we have $g = b_0 - \sigma^{-5r} \tau + \dots$, for some constant b_0 . A further consideration of the transformed version of equation (7a) shows that, to leading order,

$$\phi \sim \left(\frac{\alpha b_0}{m} \right)^{1/2} \tau \quad \text{as } \tau \rightarrow \infty.$$

To find the value of r we need to consider the outer region. The forms for f and g show that θ is of $O(\sigma^{4r})$ in this outer region and we put

$$f = \sigma^\gamma \Phi, \quad \theta = \sigma^{4r} G, \quad Y = \sigma^\delta \eta, \tag{22b}$$

for some constants γ and δ to be found. From the above, $\Phi \sim \sigma^{2r-\delta-\gamma} Y + \dots$, $G \sim b_0 - \sigma^{-4r-\delta} Y + \dots$ for small Y , giving $\delta + \gamma = 2r$ and $\delta = -4r$. The further requirement that all the terms in equation (7b) should balance gives $\gamma + 1 = \delta$. From which it follows that $r = -\frac{1}{10}$, $\delta = \frac{2}{5}$ and $\gamma = -\frac{3}{5}$.

The above discussion leads us to write, for the inner region,

$$f = \sigma^{-1/10} \phi, \quad \theta = \sigma^{-2/5} g, \quad \tau = \sigma^{-1/10} \eta, \tag{22c}$$

with equations (7) becoming

$$\phi''' + \alpha g + \frac{1}{2} (m + 1) \phi \phi'' - m \phi'^2 + m \sigma^{2/5} = 0, \tag{23a}$$

$$g'' + \sigma \left(\frac{1}{2} (m + 1) \phi g' + (1 - 2m) \phi' g \right) = 0, \tag{23b}$$

and boundary conditions (8) giving

$$\phi(0) = 0, \quad \phi'(0) = 0, \quad g'(0) = -\sigma^{1/2}. \tag{24}$$

(The outer boundary conditions have to be relaxed at this stage.)

The form of equations (23) and boundary conditions (24) suggests looking for a solution by expanding,

$$\phi(\tau; \sigma) = \phi_0(\tau) + \sigma^{2/5} \phi_1(\tau) + \sigma^{1/2} \phi_2(\tau) + \dots, \tag{25}$$

$$g(\tau; \sigma) = g_0(\tau) + \sigma^{2/5} g_1(\tau) + \sigma^{1/2} g_2(\tau) + \dots.$$

At leading order we obtain

$$g_0'' = 0. \tag{26a}$$

The solution satisfying (24) is

$$g_0 = b_0, \tag{26b}$$

for some constant b_0 which will be determined by the matching with the outer region. Equation (23a) then gives

$$\phi_0''' + \alpha b_0 + \frac{1}{2} (m + 1) \phi_0 \phi_0'' - m \phi_0'^2 = 0. \tag{27}$$

Applying the transformation $\phi_0 = (\alpha b_0 / m^3)^{1/4} \bar{\phi}_0$, $\bar{\tau} = (\alpha b_0 m)^{1/4} \tau$ to equation (27) gives

$$\bar{\phi}_0''' + 1 + \left(\frac{m + 1}{2m} \right) \bar{\phi}_0 \bar{\phi}_0'' - \bar{\phi}_0'^2 = 0 \tag{28}$$

(primes denote differentiation with respect to $\bar{\tau}$), and leaves the boundary conditions unchanged. Equation (28) is essentially the same as the leading-order equation for the inner region in the related free convection problem [10] with then,

$$\bar{\phi}_0 \sim \bar{\tau} + C_0 \tag{29}$$

as $\bar{\tau} \rightarrow \infty$. Equation (28) can now be solved numerically without needing the value of b_0 . From [10] we have, for $m = \frac{3}{5}$ (uniform plate temperature), $\bar{\phi}_0''(0) = 1.25913$ and $C_0 = -0.61782$.

Note that the transformation used to obtain this result requires α to be positive. We will return to this point later on, assuming for the present that $\alpha > 0$.

At $O(\sigma^{2/5})$ we have, from equation (23b),

$$g_1'' = 0, \quad g_1'(0) = 0, \quad (30a)$$

with solution

$$g_1 = b_1, \quad (30b)$$

and at $O(\sigma^{1/2})$ we have

$$g_2'' = 0, \quad g_2'(0) = -1, \quad (31a)$$

so that

$$g_1 = -\tau + b_2 \quad (31b)$$

for constants b_1 and b_2 .

We now have sufficient information from the inner region to obtain the leading-order behaviour of the solution and we now turn to the outer region, where, as discussed above, we put

$$f = \sigma^{-3/5}\Phi, \quad \theta = \sigma^{-2/5}G, \quad Y = \sigma^{2/5}\eta, \quad (32)$$

with equations (7) becoming,

$$\alpha G + \frac{1}{2}(m+1)\Phi\Phi'' - m\Phi'^2 + m\sigma^{2/5} + \sigma\Phi''' = 0, \quad (33a)$$

$$G'' + \frac{1}{2}(m+1)\Phi G' + (1-2m)\Phi' G = 0 \quad (33b)$$

(primes now denote differentiation with respect to Y). The outer boundary conditions are

$$G \rightarrow 0, \quad \Phi' \rightarrow \sigma^{1/5} \quad \text{as } Y \rightarrow \infty \quad (34a)$$

and, on matching with the inner region, using (26b), (29), (30b) and (31b), that

$$G \sim b_0 - Y + \dots + \sigma^{2/5}(b_1 + \dots) + \dots, \quad (34b)$$

$$\Phi \sim \left(\frac{\alpha b_0}{m}\right)^{1/2} Y + \dots \quad (34c)$$

for $Y \ll 1$.

The leading-order terms (Φ_0, G_0) in an expansion in powers of σ then satisfy the equations

$$\alpha G_0 + \frac{1}{2}(m+1)\Phi_0\Phi_0'' - m\Phi_0'^2 = 0, \quad (35a)$$

$$G_0'' + \frac{1}{2}(m+1)\Phi_0 G_0' + (1-2m)G_0\Phi_0' = 0 \quad (35b)$$

with

$$G'_0 \rightarrow 0, \quad \Phi'_0 \rightarrow 0 \quad \text{as } Y \rightarrow \infty, \tag{36a}$$

$$G_0 \sim b_0 - Y + \dots, \quad \Phi_0 \sim \left(\frac{\alpha b_0}{m}\right)^{1/2} Y + \dots. \tag{36b}$$

for $Y \ll 1$. The system given by (35) and (36) can be transformed into the same equations for the outer region solved in [10] for the analogous free convection problem. To do this we put

$$G_0 = \alpha^{-1/5} \bar{G}_0, \quad \Phi_0 = \alpha^{1/5} \bar{\Phi}_0, \quad \bar{Y} = \alpha^{1/5} Y, \quad b_0 = \alpha^{-1/5} \bar{b}_0. \tag{37}$$

Equations (35) become

$$\bar{G}_0 + \frac{1}{2} (m + 1) \bar{\Phi}_0 \bar{\Phi}_0'' - m \bar{\Phi}_0'^2 = 0, \tag{38a}$$

$$\bar{G}_0'' + \frac{1}{2} (m + 1) \bar{\Phi}_0 \bar{G}_0' + (1 - 2m) \bar{\Phi}_0' \bar{G}_0 = 0, \tag{38b}$$

with the matching conditions (36) giving

$$\bar{G}_0 \sim \bar{b}_0 - \bar{Y} + \dots, \quad \bar{\Phi}_0 \sim \left(\frac{b_0}{m}\right)^{1/2} \bar{Y} + \dots \tag{38c}$$

for $Y \ll 1$. Equations (38) are now the same as those for which a numerical solution was given in [10], if we identify m with the parameter λ used in [10] via $m = (2\lambda + 3)/5$ (or $\lambda = (5m - 3)/2$).

The solution of (38) then determines the constant \bar{b}_0 , where, from [10], $\bar{b}_0 = 1.31411$ and $\bar{\Phi}_0(\infty) = 1.37056$ for $m = \frac{3}{5}$. Note that the behaviour of Φ_0 for Y small involves a term of $O(Y^{(5m+1)/(m+1)})$ which, in turn, requires that the expansion in the inner region be modified to include a term of $O(\sigma^{2m/(m+1)})$.

From the above, we have, for $m = \frac{3}{5}$ (and then $\alpha = 1$),

$$f''(0) = (\alpha b_0)^{3/4} m^{-1/4} \bar{\Phi}_0''(0) \sigma^{-3/10} + \dots = 1.7559 \sigma^{-3/10} + \dots, \tag{39a}$$

$$\theta(0) = b_0 \sigma^{-2/5} + \dots = 1.3141 \sigma^{-2/5} + \dots. \tag{39b}$$

Graphs of $f''(0)$ and $\theta(0)$ obtained from numerical integrations of equations (7), with $\alpha = 1$ and $m = \frac{3}{5}$, are shown in Figs 3 and 4 respectively (by the full lines) together with the corresponding asymptotic forms (39) (shown by the broken lines). Both of these figures show a good agreement between (39) and the numerically determined values and act as a confirmation of the above theory.

It is interesting to note that the situation for mixed convection at small Prandtl number is quite different to that at large Prandtl number. In the latter case, the basic (leading order) solution is the purely forced convection solution, whereas in the former case, the leading-order solution is the purely free convection solution. The effect of the outer flow first appears at $O(\sigma^{1/5})$ through the outer boundary condition (34a), giving rise to a velocity ‘overshoot’ at small Prandtl numbers of $O(\sigma^{-1/5})$. This can be seen in Fig. 5, where we plot

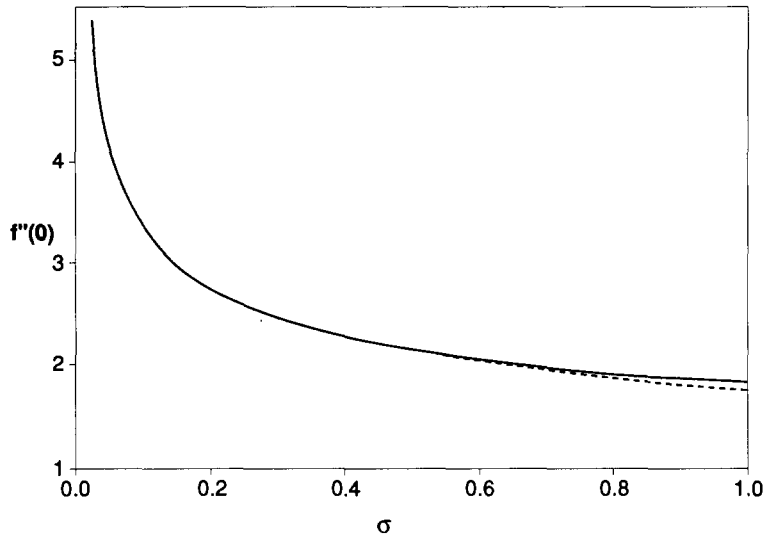


Fig. 3. A plot of $f''(0)$ obtained from the numerical solution of equations (7) for $m = 3/5$ and $\alpha = 1$ (shown by the full line). The asymptotic result for small σ , as given by (39a), is shown by the broken line.

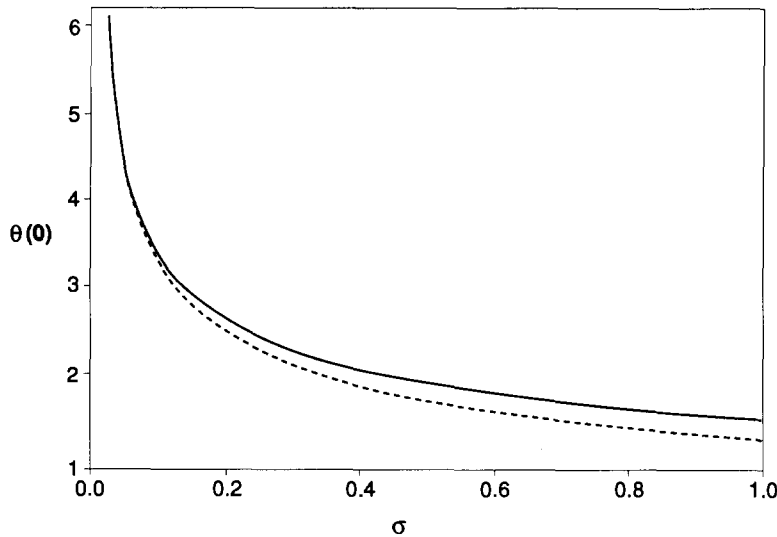


Fig. 4. A plot of $\theta(0)$ obtained from the numerical solution of equations (7) for $m = 3/5$ and $\alpha = 1$ (shown by the full line). The asymptotic result for small σ , as given by (39b), is shown by the broken line.

f' against η for $\sigma = 0.1, 0.05$ and 0.02 (and $\alpha = 1, m = \frac{3}{5}$), obtained from the numerical solution of equations (7). The increasing ‘overshoot’ as σ is decreased is clearly seen.

The above analysis was worked out on the assumption that $\alpha > 0$. Here we consider the behaviour of the solution of equations (7) for both α and σ small. A consideration of these equations for $\alpha = 0$ (when equation (7b) becomes uncoupled from equation (7a)) reveals that the scalings for the inner and outer regions are different in this case. Now there is an inner region in which η is left unscaled and θ is of $O(\sigma^{-1/2})$ and an outer region of thickness of

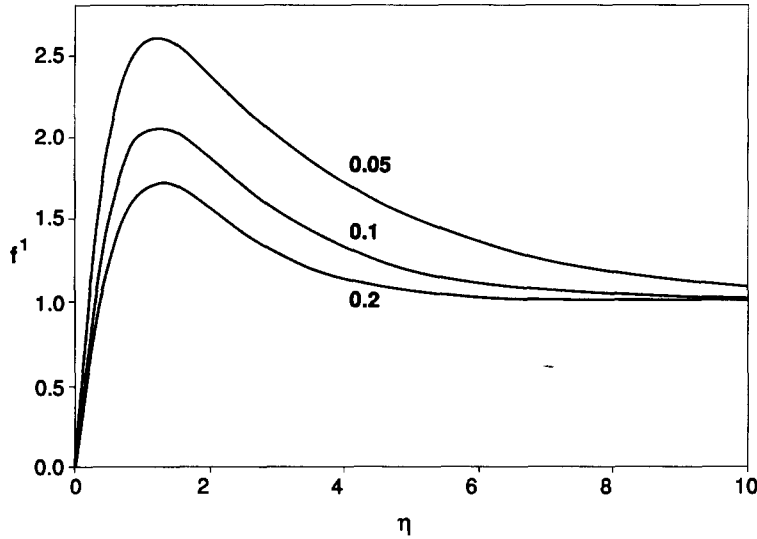


Fig. 5. Plots of $f'(\eta)$ obtained from the numerical solution of equations (7) for $\sigma = 0.2, 0.1$ and 0.05 .

$O(\sigma^{-1/2})$, and in which θ is again of $O(\sigma^{-1/2})$. With $\alpha \neq 0$ this structure will still hold provided α is of $O(\sigma^{1/2})$. So to discuss the behaviour of equations (7) for both α and σ small we put

$$\alpha = \sigma^{1/2}\beta, \tag{40}$$

where β is now of $O(1)$.

In the inner region we leave f and η unscaled and write

$$\theta = \sigma^{-1/2}P(\eta). \tag{41}$$

Equations (7) become, using (40),

$$f''' + \beta P + \frac{1}{2}(m+1)ff'' + m(1-f'^2) = 0, \tag{42a}$$

$$P'' + \sigma\left(\frac{1}{2}(m+1)fP' + (1-2m)f'P\right) = 0, \tag{42b}$$

with boundary conditions (8) giving

$$P'(0) = -\sigma^{1/2}. \tag{42c}$$

The form of boundary condition (42c) suggests that we should look for a solution by expanding,

$$f(\eta; \sigma) = f_0(\eta) + \sigma^{1/2}f_1(\eta) + \dots, \tag{43}$$

$$P(\eta; \sigma) = P_0(\eta) + \sigma^{1/2}P_1(\eta) + \dots.$$

At leading order we have

$$P_0'' = 0, \quad P_0'(0) = 0, \tag{44}$$

with solution,

$$P_0 = C_0, \tag{45}$$

for some constant C_0 to be determined. On using (45) in equation (42a) we get

$$f_0''' + \beta C_0 + \frac{1}{2}(m+1)f_0 f_0'' + m(1-f_0'^2) = 0. \tag{46}$$

Applying the transformation

$$f_0 = \left(\frac{\beta C_0 + m}{m}\right)^{1/4} \bar{f}_0, \quad \bar{\eta} = \left(\frac{\beta C_0 + m}{m}\right)^{1/4} \eta, \tag{47}$$

to equation (46) then gives

$$\bar{f}_0''' + \frac{1}{2}(m+1)\bar{f}_0 \bar{f}_0'' + m(1-\bar{f}_0'^2) = 0 \tag{48a}$$

with boundary conditions,

$$\bar{f}_0(0) = 0, \quad \bar{f}'(0) = 0. \tag{48b}$$

Equation (48) is just the Falkner–Skan problem for a given value of m and can be solved to give $\bar{f}_0''(0)$, which will be independent of both β and C_0 . As $\bar{\eta} \rightarrow \infty$, $\bar{f}_0 \sim \bar{\eta} + \delta_0 + \dots$.

At $O(\sigma^{1/2})$ we have

$$P_1'' = 0, \quad P_1'(0) = -1, \tag{49}$$

with solution

$$P_1 = -\eta + C_1. \tag{50}$$

Equation (42a) then gives

$$f_1'' + \beta(-\eta + C_1) + \frac{1}{2}(m+1)(f_0 f_1'' + f_1 f_0'') - 2m f_0' f_1' = 0. \tag{51}$$

A consideration of the behaviour of equation (51) for $\eta \gg 1$ shows that

$$\begin{aligned} f_1 &\sim \beta \left(\frac{m}{\beta C_0 + m}\right)^{1/2} \frac{\eta^2}{(1-3m)} + \dots, & m \neq \frac{1}{3}, \\ f_1 &\sim \frac{3\beta}{4} \left(\frac{m}{\beta C_0 + m}\right)^{1/2} \eta^2 \log \eta + \dots, & m = \frac{1}{3}. \end{aligned} \tag{52}$$

We now turn to the outer region in which we put

$$f = \sigma^{-1/2}\chi, \quad \theta = \sigma^{-1/2}p, \quad \xi = \sigma^{1/2}\eta. \tag{53}$$

When (53) is substituted into equations (7) and only the leading-order terms (for small σ) retained, we obtain

$$\beta p + \frac{1}{2}(m+1)\chi\chi'' + m(1-\chi'^2) = 0, \tag{54a}$$

$$p'' + \frac{1}{2}(m+1)p'\chi + (1-2m)p\chi' = 0. \tag{54b}$$

The boundary conditions to be applied are that

$$\chi' \rightarrow 1, \quad p \rightarrow 0 \quad \text{as } \xi \rightarrow \infty, \tag{55a}$$

and, from matching with the inner region, that

$$\chi \sim \left(\frac{\beta C_0 + m}{m}\right)^{1/2} \xi + \dots, \quad p \sim C_0 - \xi + \dots \tag{55b}$$

for $\xi \ll 1$. (We note that, as in the previous case, there is also a term of $O(\xi^{5/2})$ in (55b).) It is the solution of the problem given by equations (54) and boundary conditions (55) that determines the value of the constant C_0 for given values of m and β . This has to be done numerically, and a graph of C_0 against β is shown in Fig. 6, where we can see that C_0 decreases as β is increased.

The behaviour for β large can be obtained by putting

$$\chi = \beta^{1/5}\bar{\chi}, \quad p = \beta^{-1/5}\bar{p}, \quad \bar{\xi} = \beta^{1/5}\xi, \quad C_0 = \beta^{-1/5}\bar{C}_0. \tag{56}$$

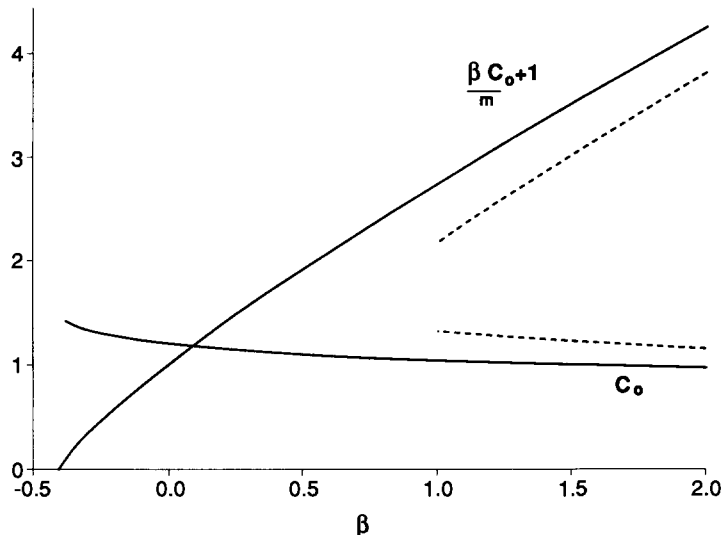


Fig. 6. Graphs of C_0 and $\beta C_0/m + 1$ (as defined in (45)) for $m = 3/5$.

Then, letting $\beta \rightarrow \infty$ leads to

$$\bar{p} + \frac{1}{2}(m+1)\bar{\chi}\bar{\chi}'' - m\bar{\chi}'^2 = 0, \tag{57a}$$

$$\bar{p}'' + \frac{1}{2}(m+1)\bar{\chi}\bar{p}' + (1-2m)\bar{p}\bar{\chi}' = 0, \tag{57b}$$

with

$$\bar{\chi} \sim \left(\frac{\bar{C}_0}{m}\right)^{1/2} \bar{\xi} + \dots, \quad \bar{p} = \bar{C}_0 - \bar{\xi} + \dots \tag{58}$$

for small $\bar{\xi}$, and

$$\bar{\chi}' = O(\beta^{-2/5}) \rightarrow 0, \quad \bar{p} \rightarrow 0 \quad \text{as } \bar{\xi} \rightarrow \infty. \tag{59}$$

The system given by (57), (58) and (59) is now the free convection problem, and using the results given previous by in [10], we have $\bar{C}_0 = 1.31411$ (for $m = \frac{3}{5}$). Graphs of $C_0 = 1.31411 \beta^{-1/5}$ and $\beta(C_0/m) + 1 = 2.1902 \beta^{4/5}$ are also shown in Fig. 6 (by the broken lines). This completes the discussion for the leading-order problem.

From (41) and (47) we have

$$f''(0) = \left(\frac{\beta C_0}{m} + 1\right)^{3/4} \bar{f}''_0(0) + \dots, \tag{60a}$$

$$\theta(0) = C_0 \sigma^{-1/2} + \dots, \tag{60b}$$

where $\bar{f}''_0(0)$ depends only on m . A graph of $\beta C_0/m + 1$ (for $m = \frac{3}{5}$) is also shown in Fig. 6. From this graph we can see that the expression $\beta C_0/m + 1 \rightarrow 0$ as β is decreased, becoming zero at $\beta \approx -0.4$. Hence, from (60a), $f''(0)$ will also be zero at this value of β , with the form of the transformation (47) suggesting that the solution cannot be continued beyond this point.

However, we know from [16] that there is a value of α , α_s (say), which depends on σ , at which the solution terminates with $f''(0) = 0$ there. (In [16] we found two branches of solution in $\alpha_s < \alpha < 0$ for $\sigma = 1$.) To complete the discussion, we calculate the value of α_s for small σ . To do this we have to solve equations (7), subject to boundary conditions (8) together with the extra condition that $f''(0) = 0$ at $\alpha = \alpha_s$. As above we will have,

$$\alpha_s = \sigma^{1/2} \beta_s, \tag{61}$$

but the scalings for the inner region will be different to the small α case described above. To calculate these we note that, for $\eta \ll 1$, $\theta \approx d_0 \sigma^{-1/2} - \eta + \dots$, for some constant d_0 . When this is substituted into equation (7a) we find we must have $m + d_0 \beta_s = 0$, and a balancing of buoyancy force (now proportional to $\sigma^{1/2} \eta$), convective and viscous terms leads us to write, for the inner region,

$$f = \sigma^{1/10} S, \quad \theta = \sigma^{-1/2} Q, \quad \rho = \sigma^{1/10} \eta. \tag{62}$$

Equations (7) become,

$$\beta_s Q + m + \sigma^{2/5} \left(S''' + \frac{1}{2} (m+1) S S'' - m S'^2 \right) = 0, \quad (63a)$$

$$Q'' + \sigma \left(\frac{1}{2} (m+1) S Q' + (1-2m) S' Q \right) = 0, \quad (63b)$$

subject to the boundary conditions that,

$$S(0) = 0, \quad S'(0) = 0, \quad S''(0) = 0, \quad Q'(0) = -\sigma^{2/5}. \quad (64)$$

The form of (64) suggest an expansion of the form

$$S(\rho; \sigma) = S_0(\rho) + \sigma^{2/5} S_1(\rho) + \dots, \quad Q(\rho; \sigma) = Q_0(\rho) + \sigma^{2/5} Q_1(\rho) + \dots. \quad (65)$$

At leading order, we have

$$Q_0'' = 0, \quad Q_0'(0) = 0. \quad (66a)$$

Hence,

$$Q_0 = d_0, \quad (66b)$$

for some constant d_0 . Using this in equation (63a) gives,

$$\beta_s d_0 + m = 0. \quad (67)$$

At $O(\sigma^{2/5})$ we have

$$Q_1'' = 0, \quad Q_1'(0) = -1, \quad (68a)$$

giving

$$Q_1 = -\rho + d_1. \quad (68b)$$

Using (68b) in equation (63a) then gives

$$S_0''' + \frac{1}{2} (m+1) S_0 S_0'' - m S_0'^2 + \beta_s (-\rho + d_1) = 0. \quad (69)$$

This equation has to be solved subject to

$$S_0(0) = 0, \quad S_0'(0) = 0, \quad S_0''(0) = 0. \quad (70)$$

However, it is the behaviour of the solution as $\rho \rightarrow \infty$ that we require. A consideration of equation (69) shows that

$$S_0 \sim \left(\frac{-8\beta_s}{3(5m-1)} \right)^{1/2} \rho^{3/2} + \dots, \quad \text{as } \rho \rightarrow \infty. \quad (71)$$

The scalings for the outer region are the same as for the small α solution. These are given

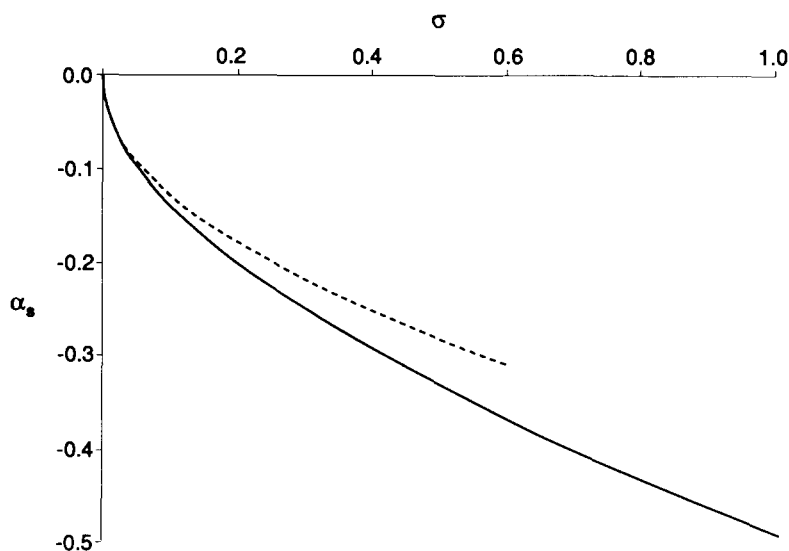


Fig. 7. The bifurcation value α_s plotted against σ . The asymptotic result (61) for small σ , with $\beta_s = -0.40256$, is shown by the broken line.

by (53), with the resulting (leading order) equations again given by (54) (with β_s replaced by β). The outer boundary conditions are still the same (given by (55a)), but now we have, for $\xi \ll 1$,

$$p \sim d_0 - \xi + \dots, \quad \chi \sim \left(\frac{-8\beta_s}{3(5m-1)} \right)^{1/2} \xi^{3/2} + \dots \tag{72}$$

The solution of the equations in the outer region, subject to (72), then determines the value of β_s (and hence d_0 via (67)). Again this has to be done numerically and we find that $\beta_s = -0.40256$ (for $m = \frac{3}{5}$). The results are shown in Fig. 7, where we give a plot of α_s against σ (for $m = \frac{3}{5}$), shown by the full line. Here α_s has been obtained from a numerical integration of the basic problem, i.e. equations (7) with α replaced by α_s and the extra boundary condition $f''(0) = 0$ applied. The result for $\sigma = 1$ was given in [16]. Also shown in Fig. 7 (by the broken line) is a graph of the asymptotic result $\alpha_s = -0.40256 \sigma^{1/2}$. This figure shows a good agreement between the two results for small σ . Now, from [16], a solution of equation (7) exists only for $\alpha \geq \alpha_s$ and, as seen above, $\alpha_s \rightarrow 0$ like $\sigma^{1/2}$ as $\sigma \rightarrow 0$. Hence the range of negative α (opposing flow) over which a solution to the similarity equations (7) exists decreases to zero as $\sigma \rightarrow 0$.

Finally, we can see that the solution obtained for α of $O(1)$, as $\alpha \rightarrow 0$, overlaps that obtained for α small as $\beta (= \sigma^{-1/2}\alpha) \rightarrow \infty$. If we substitute $\alpha = \beta\sigma^{1/2}$ and, from (37), $\bar{b}_0 = \alpha^{-1/5}b_0$, (with \bar{b}_0 given by (38)) into (39), we obtain $f''(0) = \beta^{3/5}(b_0/m)^{3/4}m^{1/2}\bar{\phi}_0''(0) + \dots$ and $\theta(0) = \bar{b}_0\beta^{-1/5}\sigma^{-1/2} + \dots$, which agree with the solution for $\beta \gg 1$ as given by (56), (57), (58) and (59).

4. General boundary-layer flow

Here we use the scalings derived above for the similarity equations (7) to discuss the nature of solutions of equations (3) for small and large values of σ . We consider the flow of a

uniform stream over a vertical flat plate with a constant surface heat as a flux particular example. This problem has previously been discussed in some detail by Wilks [14, 15] and Hunt and Wilks [17] for Prandtl numbers of order unity.

(a) *Large Prandtl numbers*

The discussion in the previous section suggests that for this case we write

$$\psi = \sigma^{-2/3}\Psi, \quad T = \sigma^{-1/3}\theta, \quad Y = \sigma^{1/3}y \quad (73)$$

for the inner layer. Equations (3) then become

$$\frac{\partial^3\Psi}{\partial Y^3} + \sigma^{-1/3}U \frac{dU}{dx} + \sigma^{-2/3}\alpha\theta + \sigma^{-1}\left[\frac{\partial\Psi}{\partial x} \frac{\partial^2\Psi}{\partial Y^2} - \frac{\partial\Psi}{\partial Y} \frac{\partial^2\Psi}{\partial x \partial Y}\right] = 0, \quad (74a)$$

$$\frac{\partial^2\theta}{\partial Y^2} + \frac{\partial\Psi}{\partial x} \frac{\partial\theta}{\partial Y} - \frac{\partial\Psi}{\partial Y} \frac{\partial\theta}{\partial x} = 0, \quad (74b)$$

subject to boundary conditions

$$\Psi = 0, \quad \frac{\partial\Psi}{\partial Y} = 0, \quad \frac{\partial\theta}{\partial Y} = -1 \quad \text{on } Y = 0. \quad (75)$$

Equation (74a) shows that to leading order

$$\Psi = \frac{1}{2} a_0(x) Y^2, \quad (76)$$

for some function $a_0(x)$ to be determined. Equation (74b) then becomes, using (76),

$$\frac{\partial^2\theta}{\partial Y^2} + a_0' \frac{Y^2}{2} \frac{\partial\theta}{\partial Y} - a_0 Y \frac{\partial\theta}{\partial x} = 0. \quad (77)$$

Equation (77) is to be solved subject to boundary condition (75) and that $\theta \rightarrow 0$ as $Y \rightarrow \infty$.

In the outer region we have $\theta \equiv 0$, and ψ and y are left unscaled, so that the solution is then given by equations (3a) and (3b). This is the forced flow solution for the particular outer flow $U(x)$, as the matching with the inner region gives $\psi \sim a_0 y^2/2$ for y small. The solution of this boundary-layer problem for the given $U(x)$ determines the function $a_0(x)$ and we can then return to the inner region and complete the solution of equation (77).

The boundary condition on $Y = 0$ appears to preclude us from transforming equation (77) into a simple heat conduction problem, as was done previously by Kuiken [19] for a similar problem. However, equation (77) has a simple solution when $a_0(x)$ is given by $a_0(x) = A_0 x^r$ for some power r . On writing

$$\theta = x^{(1-r)/3} h(\zeta), \quad \zeta = Y x^{(r-1)/3}, \quad (78)$$

equation (77) reduces to the ordinary differential equation

$$h'' + \frac{A_0}{6} (r+2) \zeta^2 h' - \frac{A_0}{3} (1-r) \zeta h = 0, \quad (79)$$

subject to the boundary conditions

$$h'(0) = -1, \quad h(\infty) = 0. \quad (80)$$

The solution of equation (79) can be written in terms of confluent hypergeometric functions [18] as

$$h = \frac{\Gamma\left(\frac{2}{r+2}\right)}{3\Gamma\left(\frac{2}{3}\right)} \left(\frac{18}{(r+2)A_0}\right)^{1/3} e^{-wU} \left(\frac{2}{2+r}; \frac{2}{3}; w\right), \quad (81)$$

where $w = (A_0/18)(r+2)\zeta^3$. From (81) it then follows that the plate temperature T_w is given by

$$T_w = \frac{\Gamma\left(\frac{2}{r+2}\right)\Gamma\left(\frac{1}{3}\right)}{3\Gamma\left(\frac{2}{3}\right)\Gamma\left(\frac{r+8}{3(2+r)}\right)} \left(\frac{18}{(r+2)A_0}\right)^{1/3} x^{(1-r)/3} \sigma^{-1/3} + \dots. \quad (82a)$$

For the particular example of a uniform stream, $\psi = x^{1/2}f(\eta)$, $\eta = y/x^{1/2}$, where f satisfies the well-known Blasius equation. For $\eta \ll 1$, $f \sim \frac{1}{2}A_0\eta^2 + \dots$, where $A_0 = 0.33206$, so that for $y \ll 1$, $\psi \sim \frac{1}{2}A_0y^2/x^{1/2}$ and hence $a_0(x) = A_0x^{-1/2}$.

On using this in (82a) we find that, for this case, the plate temperature is given by

$$T_w = \frac{1}{6} \left(\frac{12}{A_0}\right)^{1/3} \frac{(\Gamma(1/3))^2}{(\Gamma(2/3))^2} x^{1/2} \sigma^{-1/3} + \dots = 2.1567x^{1/2} \sigma^{-1/3} + \dots. \quad (82b)$$

To examine this problem further, we solved the governing equations numerically for a range of values of σ . The equations for this case are [14, 15]

$$\frac{\partial^3 \psi}{\partial y^3} \pm T + \frac{\partial \psi}{\partial x} \frac{\partial^2 \psi}{\partial y^2} - \frac{\partial \psi}{\partial y} \frac{\partial^2 \psi}{\partial x \partial y} = 0, \quad (83a)$$

$$\frac{\partial^2 T}{\partial y^2} + \sigma \left(\frac{\partial \psi}{\partial x} \frac{\partial T}{\partial y} - \frac{\partial \psi}{\partial y} \frac{\partial T}{\partial x} \right) = 0, \quad (83b)$$

subject to the boundary conditions that

$$\psi = 0, \quad \frac{\partial \psi}{\partial y} = 0, \quad \frac{\partial T}{\partial y} = -1 \quad \text{on } y = 0; \quad \frac{\partial \psi}{\partial y} \rightarrow 1, \quad T \rightarrow 0 \quad \text{as } y \rightarrow \infty. \quad (84)$$

(the + sign in equation (83a) refers to the aiding case – buoyancy forces and flow in the same direction – and the – sign to the opposing case). As in [14, 15], to start the solution of equations (83) at the leading edge $x = 0$, a transformation of variables is required, given by

$$\psi = x^{1/2}f(\eta, x), \quad \theta = x^{1/2}h(\eta, x), \quad \eta = y/x^{1/2}. \quad (85)$$

Transformation (85) was first applied to (83) and the resulting equations were then solved by

essentially the same method as described by Mahmood and Merkin [20]. The method is described fully in [20] and the details need not be repeated here. Care had to be taken to use a sufficiently small step length $\Delta\eta$ in the η -direction, as for the larger values of σ , the thermal layer became increasingly confined to a narrower region close to the plate (in line with the analysis described above). For $\sigma = 1$, a value of $\Delta\eta = 0.05$ was found to give satisfactory accuracy (4 figures or better), but this had to be reduced to $\Delta\eta = 0.02$ for $\sigma = 100$, (the largest value of σ taken).

The analysis presented above shows that as σ is increased, the flow approaches the forced convection limit, which, in this case, is the Blasius boundary-layer solution. To show as clearly as possible that this is in fact the case, we have plotted a skin friction parameter $C_f = x^{1/2}(\partial^2\psi/\partial y^2)_{y=0} = (\partial^2f/\partial\eta^2)_{\eta=0}$ against x in Fig. 8 for the aiding case. The theory suggests that $C_f \rightarrow A_0 = 0.33206$ for all x as $\sigma \rightarrow \infty$, and we can see that this appears to be the case. All the curves start with $C_f = A_0$ at $x = 0$, and become flatter for the larger values of σ . Also, from (82), the plate temperature T_w is of $O(\sigma^{-1/3})$ and to see how this behaves as σ is increased, we have plotted $x^{-1/2}\sigma^{1/3}T_w = T_w^{(a)}$ against x for a range of values of σ in Fig. 9. Again the above theory requires that these curves should become flatter, with $T_w^{(a)} \rightarrow 2.1567$ for all x , as σ is increased. Again, we can see that this appears to be the case from the graphs given in Fig. 9.

For large Prandtl number the heat transfer mechanism is essentially by forced convection, with the heat supplied to the fluid through the plate having an increasingly less significant effect. This should manifest itself for the opposing case by delaying the onset of separation, and, to check that this is the case, we also obtained numerical solutions of equations (83) for the opposing case. The results are summarised in Fig. 10, where we give a plot of the separation point x_s against σ (x_s is where the skin friction becomes zero).

We can consider equations (83) further and get an estimate for the values of x when the natural convective effects will start to influence the flow. To do this we now have to scale x , and, on writing $\bar{x} = \sigma'x$, a balancing of terms in equation (83a) and boundary condition (84)

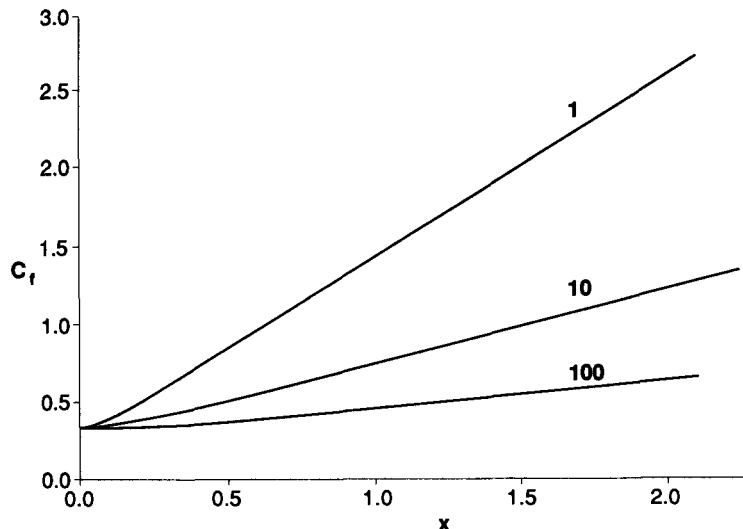


Fig. 8. The skin friction parameter $C_f = x^{1/2}(\partial^2\psi/\partial y^2)_{y=0}$, obtained from the numerical solution of equations (83) for the aiding case, plotted against x , for $\sigma = 1, 10, 100$.

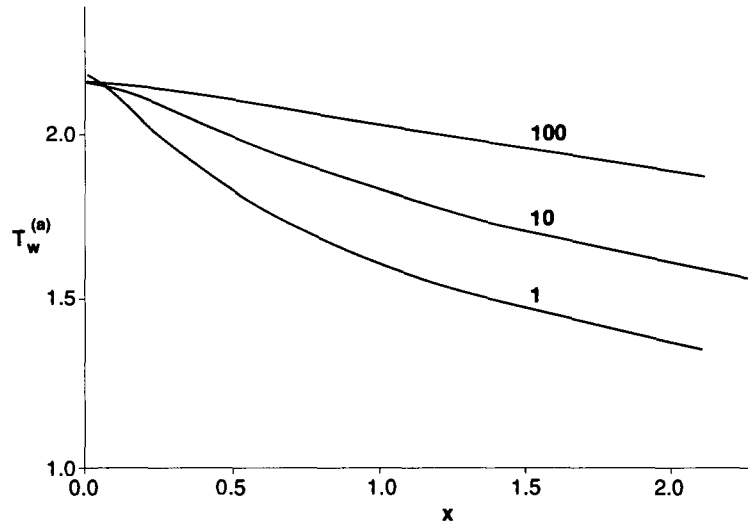


Fig. 9. The modified plate temperature $T_w^{(a)} = \sigma^{1/3}x^{-1/2}T_w$, obtained from the numerical solution of equations (83) for the aiding case, plotted against x , for $\sigma = 1, 10, 100$.

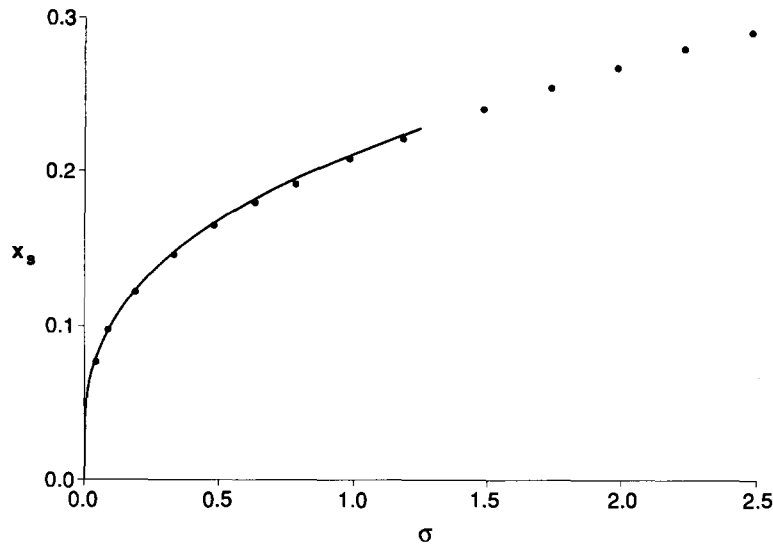


Fig. 10. The separation point x_s obtained from the numerical solution of equations (83) for the opposing case (shown by \cdot). The estimated form (91) for small σ is shown by the full line.

requires that for the inner region we put

$$\psi = \sigma^{-4(1+r)/5}\bar{\psi}, \quad T = \sigma^{-(1+r)/5}\bar{T}, \quad \bar{y} = \sigma^{(1+r)/5}y. \tag{86a}$$

At the outer edge of this inner region, $\psi \sim a_0(\bar{x})\bar{y}$, $\bar{T} \rightarrow 0$. In the outer region, where the buoyancy force term is to be neglected, a balancing of convective and viscous terms, as well as boundary condition (84), suggests that we put

$$\psi = \sigma^{-r/2}\bar{\Psi}, \quad \bar{Y} = \sigma^{r/2}y. \tag{86b}$$

The matching requirement on ψ then gives $r = -1$, and hence, for the buoyancy force to have an influence, at leading order, on the flow, we must scale x by

$$\bar{x} = \sigma^{-1}x. \quad (87)$$

With this scaling for x , (86a) shows that the inner region is left unscaled, while in the outer region ψ is $O(\sigma^{-1/2})$ and y is $O(\sigma^{1/2})$. Also, it is worth noting that with this scaling for x applied to the transformation of variables (6b) to obtain the similarity equations (7), for $m = \frac{3}{5}$, we obtain the scalings for the inner and outer regions given originally by Roy [8] for the high Prandtl number limit. (87) shows that the effect of the buoyancy forces will be felt only when x is of $O(\sigma)$, so that, although for the aiding case natural convection will be the dominant heat transfer mechanism well downstream from the leading edge, this will come into play at increasingly longer distances downstream as σ is increased. (87) also suggests that, for the opposing case, the onset of separation will become increasingly delayed as σ is increased, as is seen in Fig. 10.

(b) Small Prandtl numbers

Here we are able to get less detailed information for the general boundary-layer flow than is possible for the high Prandtl number limit. The scalings implied by (22c), when applied to the boundary-layer equations (3), lead to an inner region in which

$$T = B_0(x)\sigma^{-2/5} - y + \dots, \quad (88)$$

with the momentum equation involving the unknown function $B_0(x)$ (but not the free stream $U(x)$, to leading order). The scalings for the outer region are again suggested by (32), which gives natural convection equations analogous to equation (33) to leading order in this outer region, with the pressure gradient term of $O(\sigma^{2/5})$ and the free stream of $O(\sigma^{1/5})$. There is no simple solution possible for the equations in either the inner or the outer region, even for the uniform stream with uniform surface heat flux, as there was for the high Prandtl number case, and the full partial differential equations would have to be solved numerically. This is not pursued any further here.

However, we do note that the effect of reducing the Prandtl number is to enhance the effect of the buoyancy forces. This can be seen from Figs 11 and 12 where we plot C_r (as defined earlier) and a wall temperature parameter $T_\omega^{(b)} = x^{1/2}\sigma^{2/5}T_\omega$ for $\sigma = 0.05, 0.1, 0.2$ and 1.0 obtained from the numerical solution of equations (83), as described earlier. In both cases the gradients of the curves increase as σ is decreased, showing that the influence of the buoyancy forces is felt closer to the leading edge the smaller the value of σ . This effect of the increased influence of the buoyancy forces for small σ is also shown, for the opposing case, by the separation point x_s being moved closer to the leading edge. This can be seen clearly in Fig. 10.

Again we can get some estimate for the scale over which the initial forced convection behaviour will hold, as this must be a form of solution close to the leading edge, even for small σ . To do this we carry out a scaling analysis as described above for the high Prandtl number case. A balance of convective, buoyancy and viscous terms in equation (83a) suggests that, for the inner region, we write

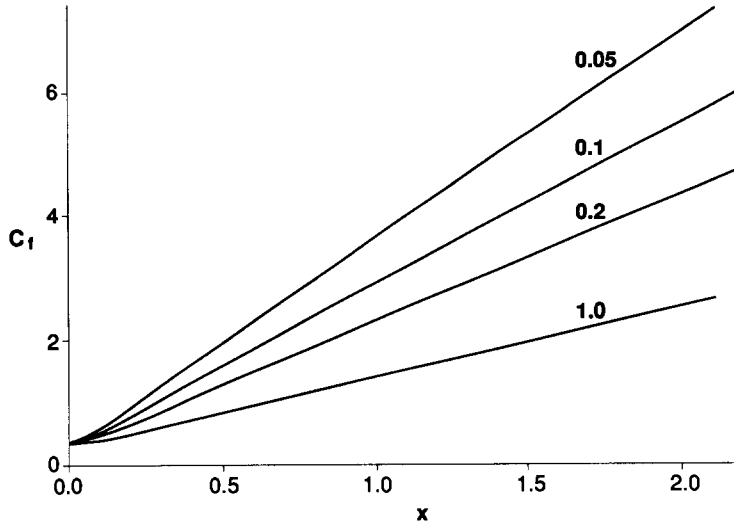


Fig. 11. The skin friction parameter $C_f = x^{1/2}(\partial^2\psi/\partial y^2)_{y=0}$, obtained from the solution of equations (83) for the aiding case, plotted against x , for $\sigma = 1, 0.2, 0.1$ and 0.05 .

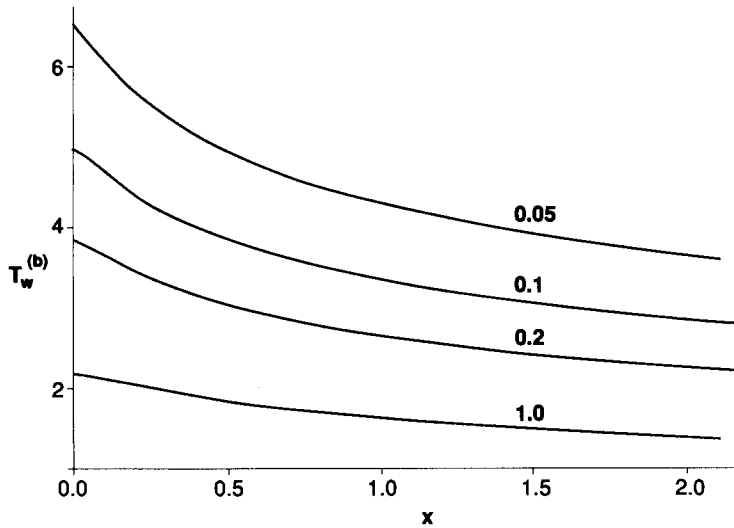


Fig. 12. The modified wall temperature $T_w^{(b)} = x^{-1/2}\sigma^{2/5}T_w$, obtained from the numerical solution of equations (83) for the aiding case, plotted against x , for $\sigma = 1, 0.2, 0.1$ and 0.05 .

$$\psi = \sigma^{s-t}\bar{\psi}, \quad T = \sigma^{4s-t}\bar{T}, \quad \bar{y} = \sigma^2 y, \tag{89a}$$

where we have assumed a scaling for x as $\bar{x} = \sigma^t x$. In the outer region we must have T again of $O(\sigma^{4s-t})$, and a balancing of all terms in equation (83b) and the convective and buoyancy force terms in equation (83a), suggests that for the outer region we write

$$\psi = \sigma^{(2s-2t-1)/2}\bar{\Psi}, \quad T = \sigma^{4s-t}\bar{\theta}, \quad \bar{Y} = \sigma^{(2s+1)/2} y. \tag{89b}$$

The requirement that $\partial\psi/\partial y$ be of $O(1)$ in the outer region, and the matching with the inner

region, where $T = \sigma^{4s-t}(C_0(x) - \sigma^{t-4s}y + \dots)$, then gives $t = 2s$ and $2t = 10s + 1$. Hence $t = -\frac{1}{3}$, (and $s = -\frac{1}{6}$), giving a scaling for x as

$$\bar{x} = \sigma^{-1/3}x. \quad (90)$$

(90) shows that the initial forced convection solution will be confined to a region of streamwise extent of $O(\sigma^{1/3})$ near the leading edge for small σ . It also suggests that the separation point x_s will move towards the leading edge with

$$x_s \sim C\sigma^{1/3}, \quad (91)$$

for $\sigma \ll 1$ where C is a constant. The value for C can be estimated from the numerical results, and a value of $C \approx 0.21$ is indicated. A graph of this is shown in Fig. 10, showing a reasonable agreement between the calculated and estimated values (from (91)) to moderately large values of σ .

5. Conclusion

We have considered the mixed convection boundary-layer flow over a vertical surface with a prescribed surface heat flux for both large and small values of the Prandtl number. The similarity equations for this problem were treated in some detail first. These showed that for large Prandtl numbers, the heat transfer is dominated by forced convection, whereas the opposite applies for low Prandtl numbers, as now it is free convection which is the dominant heat transfer process. This is, perhaps, to be expected as the Prandtl number is the ratio of the kinematic viscosity to the thermometric conductivity. A high value for the Prandtl number corresponds to a much smaller value for the thermometric conductivity in relation to the kinematic viscosity (though both will have to be small for a boundary-layer flow to be established), with the consequence that the heat transfer from the plate will have only a weak effect. The opposite is true for low values of the Prandtl number, now the heat transfer from the plate becomes the most important mechanism. The buoyancy parameter α can, however, affect this picture and estimates on α have been obtained. In the large Prandtl number range, buoyancy forces alter the leading-order behaviour when α is large, of $O(\sigma^{2/3})$, while in the small Prandtl number region, forced convection effects become important at leading order when α is small, of $O(\sigma^{1/2})$. A further consequence of this is that the range of negative buoyancy parameter (opposed flow) over which a solution can exist decreases (like $\sigma^{1/2}$) as $\sigma \rightarrow 0$.

The detailed scalings derived for the similarity equations were then used to discuss the behaviour of the solution of the general mixed convection boundary-layer equations for large and small Prandtl numbers, with the particular example of the uniform flow over a vertical flat plate with uniform surface heat flux being treated in detail. For the streamwise co-ordinate x of $O(1)$, the solution approaches the corresponding forced convection limit as $\sigma \rightarrow \infty$, whereas the solution is dominated by free convection as $\sigma \rightarrow 0$. We then showed that heat transfer from the plate becomes important when x is of $O(\sigma)$ for $\sigma \gg 1$, and that the initial forced convection solution holds only for x of $O(\sigma^{1/3})$ for $\sigma \ll 1$. This effect is seen in the opposing case as delaying the onset of separation for large σ , while the separation point is moved closer to the leading edge for small σ .

References

1. S. Ostrach, An analysis of laminar free-convection flow and heat transfer about a flat plate parallel to the direction of the generating body force, N.A.C.A. Report 1111 (1953).
2. E.M. Sparrow and J.L. Gregg, Laminar free convection from a vertical plate with uniform surface heat flux. *Trans. A.S.M.E.* 78 (1956) 435–440.
3. E.M. Sparrow and J.L. Gregg, Similar solutions for free convection from a nonisothermal vertical plate. *Trans. A.S.M.E.* 80 (1958) 379–386.
4. E.J. Lefevre, Laminar free convection from a vertical plane surface. 9th International Congress on Applied Mechanics, Brussels, paper I168 (1956).
5. K. Stewartson and L.T. Jones, The heated vertical plate at high Prandtl number. *J. Aeronautical Sciences* 24 (1957) 379–380.
6. H.K. Kuiken, An asymptotic solution for large Prandtl number free convection. *J. Engng. Math.* 2 (1968) 355–371.
7. S. Eshghy, Free convection at large Prandtl number. *J. Applied Math. and Physics (ZAMP)* 22 (1971) 275–292.
8. S. Roy, High Prandtl number free convection for uniform surface heat flux. *Trans. A.S.M.E. J. Heat Transfer* 95 (1973) 124–126.
9. H.K. Kuiken, Free convection at low Prandtl numbers. *J. Fluid Mech.* 37 (1969) 785–798.
10. J.H. Merkin, Free convection on a heated vertical plate: the solution for small Prandtl number. *J. Engng. Math.* 23 (1989) 273–282.
11. E.M. Sparrow and J.L. Gregg, Buoyancy effects in forced-convection flow and heat transfer. *J. Appl. Mech.* 81 (1959) 133–134.
12. A.A. Szewczyk, Combined forced and free-convection laminar flow. *J. Heat Transfer* 86 (1964) 501–507.
13. J.H. Merkin, The effect of buoyancy forces on the boundary-layer flow over a semi-infinite vertical flat plate in a uniform free stream. *J. Fluid Mech.* 35 (1969) 439–450.
14. G. Wilks, The flow of a uniform stream over a semi-infinite vertical flat plate with uniform surface heat flux. *Int. J. Heat Mass Transfer* 17 (1974) 743–753.
15. G. Wilks, A separated flow in mixed convection. *J. Fluid Mech.* 62 (1974) 359–368.
16. J.H. Merkin and T. Mahmood, Mixed convection boundary layer similarity solutions: prescribed wall heat flux. *J. Applied Math. and Physics (ZAMP)* 40 (1989) 51–68.
17. R. Hunt and G. Wilks, Continuous transformation computation of boundary layer equations between similarity regimes. *J. Computational Physics* 40 (1981) 478–490.
18. L.J. Slater, *Confluent hypergeometric functions*, Cambridge University Press, Cambridge (1960).
19. H.K. Kuiken, Heat or mass transfer from an open cavity. *J. Engng. Math.* 12 (1978) 129–155.
20. T. Mahmood and J.H. Merkin, Mixed convection on a vertical cylinder. *J. Applied Math. and Phys. (ZAMP)* 39 (1988) 186–203.